Synthesis of Metal Oxide Nanoparticles by Thermal Decomposition of a Ni(II) Complex and its Antimicrobial Activity

Sunil S. Patil, Vishal S. Kamble, Digambar K. Patil, Jitendra M. Pawara*
[1]Department of Chemistry, Changu Kana Thakur Arts, Commerce and Science College, New Panvel (Autonomous), Maharashtra, India
*Corresponding author (e-mail: jmpawara@gmail.com)

Aqua(2-amino-6-methyl pyrimidine-4-ol and leucine)Ni(II) complex was synthesized from nickel chloride hexahydrate ($NiCl_2 \cdot 6H_2O$) with 2-amino-6-methyl pyrimidine-4-ol (HP) as primary ligand and leucine as secondary ligand. The synthesized complex was characterized by elemental analysis, infrared (IR) spectroscopy, ultraviolet-visible (UV-vis) spectroscopy and differential thermal/thermogravimetric analysis (TG/DTA). The prepared complex was subjected to thermal decomposition at 400 °C in an oven which produced pure NiO in the form of regular spherical nanoparticles. The structure of the product was elucidated based on FT-IR, UV, TG/DTA, X-ray diffraction (XRD), scanning electron microscopy (SEM) and transmission electron microscopy (TEM). Further, the synthesized nickel oxide nanoparticles demonstrated remarkable antimicrobial activity.

Key words: Ni(II) complex; thermal decomposition; NiO nanoparticle; antimicrobial activity.

Received: July 2021; Accepted: September 2022

Nanotechnology has been a marvellous impetus in the rapidly emerging area of technology and has provided an abundance of possibilities to overcome the growing challenges of technology [1-2]. Nano-materials have been explored in numerous scientific and technological fields due to their varied applications and specific properties [3–5]. Recently metallic nanoparticles (NPs) have attracted interest, mainly because of their distinctive physical and chemical properties. These properties are conferred by their size, shape, and surface area [6–11] and can be controlled by the preparation method. One of the main effects, which evolved by controlling particle size, is their antimicrobial activity [12,13]. The antimicrobial activity of NiO NPs is known to be a function of the surface area in close contact with microorganisms.

For this reason, the high surface area of NPs ensures a vast range of reactions on the surface of microorganisms and can stop normal function of cells or result in cell death [14]. Based on the literature, there have been several methods reported for the preparation of NiO NPs including thermal decomposition [15], combustion [16], sol-gel [17] co-precipitation [18], spray pyrolysis [19], anodic arc plasma method [20], etc. The present study reports the facile straightforward synthesis; this has an advantage over other methods as it is simple, rapid, and energy-saving [21]. Herein we communicate the synthesis, characterization, and antimicrobial activity of NiO nanoparticles. The starting complex and final NiO nanoparticle product were characterized before and after thermal decomposition using Fourier transform infrared (FT-IR) spectroscopy, ultraviolet-visible (UV-vis) spectroscopy, differential thermal/thermogravimetric analysis (TG/DTA), X-ray diffraction (XRD), scanning electron microscopy (SEM) and transmission electron microscopy (TEM). The present study also reports the direct thermal decomposition process of the desired complex precursor. One of the most important and straightforward strategies is to obtain structurally elaborated and pure NiO nanoparticles with regular spherical shapes. The antimicrobial activity of the Ni(II) complex and NiO nanoparticles was also investigated.

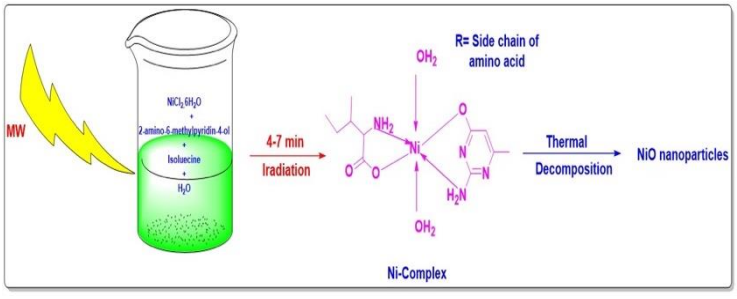

Figure 1. Schematic Representation of the Preparation of Ni(II) Complex and NiO Nanoparticles

EXPERIMENTAL SECTION

All the chemicals used in the current work were of analytical grade, procured from Aldrich, E. Merck, and S.D. Fine-Chem Ltd. Nickel (II) chloride hexahydrate was procured from E. Merck and used as obtained. L-isoleucine was obtained from S.D. Fine-Chem Ltd., Mumbai. In contrast, 2-amino-6-methyl pyrimidine-4-ol was purchased from Sigma Aldrich and imported from the United States. The solvents ethanol, methanol, dimethyl formamide (DMF), dimethyl sulfoxide (DMSO) and chloroform were distilled and purified according to standard procedures [22].

1. Physical Measurements

Nickel content was estimated complexometrically by standard protocols [23-24]. Fourier Transform infrared spectra were recorded in the spectral range of 4000-400 cm^{-1} on a Perkin Elmer FT-IR model no 1500 at IIT Bombay. UV-vis spectra were recorded in the range of 200-800 nm using a Perkin Elmer Lambda-950 UV-VIS spectrometer employing DMSO as a solvent. Thermal analysis was carried out in a controlled nitrogen atmosphere with a Perkin Elmer Diamond TG-DTA instrument. Microwave synthesis was performed in a domestic microwave oven, model KENSTAR-OM20ACF, 2450MHz, 800W. The synthesized NiO NPs were characterized by scanning electron microscopy (SEM Hitachi S-4800) and X-ray diffraction (Bruker D8 Advance X-ray diffractometer).

1.1. Synthesis of Ni(II) Complex by Microwave Method

An aqueous solution (10 cm^3) of nickel chloride hexahydrate (237 mg, 1 mmol) was added to an aqueous solution (10 cm^3) of 2-amino-6-methyl pyrimidine-4-ol (HP) (124 mg, 1 mmol). To this hot solution, an aqueous solution (10 cm^3) of L-leucine (HL) (112 mg, 1 mmol) was added with continuous stirring. The reaction mixture was heated in the microwave for about 4-7 min. The complex was obtained by raising the pH of the reaction mixture by adding aqueous ammonia. The mixture was then cooled. The solid complex obtained was filtered using a suction pump and washed with ethanol and water [25].

1.2. Synthesis of NiO Nanoparticles by Thermal Decomposition of Ni (II) Complex

Approximately 0.5 g of the *Aqua*(2-amino-6-methyl pyrimidine-4-ol and isoleucine) Ni(II) complex was heated in an oven at 800 °C for 30 min. During the reaction, a brown colour indicated the formation of NiO NPs. The resulting powder was cooled to room temperature and washed a few times with ethanol to eliminate residues; finally, the prepared NPs were dried in an oven.

1.3. Antibacterial Activity by Agar Cup Method

Using the agar cup method, a single compound can be tested against many organisms or a given organism against various concentrations of the same compound [26]. This method was found useful for liquid or semisolid samples and was used in the present work. In this technique, the chosen test strain was transferred to a plate of sterile nutrient agar at a height of about 5 mm and allowed to solidify. Then a cup of about 8 mm diameter was cut from the centre of the plate with a sterile cork borer. The cup was filled with the test solution of known concentration, and the vessel was incubated at 38 °C for 24 hours. The extent of growth inhibition from the verge of the cup was considered a measure of the activity of the given complex. Using some plates simultaneously, we quantitatively examined the activity of some samples.

RESULT AND DISCUSSION

1. Characterization of Metal Complex

The synthesis of the Ni(II) complex may be represented as follows:

$$NiCl_2.6H_2O + HP + HL \rightarrow [Ni(P)(L).2H_2O] + 2HCl + 4H_2O$$

Where HP is 2-amino-6-methyl pyrimidine-4-ol and HL is L-isoleucine. The prepared complex was light blue in colour, non-hygroscopic, and a thermally stable solid, indicating a solid metal-ligand bond. The complex was soluble to some extent in methanol, ethanol, chloroform, DMF, and DMSO. The elemental analysis data of the metal complex was consistent with the general formulation of 1:1:1, a complex of the type $[Ni(P)(L).2H_2O]$. The molar conductance values of the complex in DMF at a concentration of 10^{-3} M were low (<1), indicating their non-electrolytic nature [27].

2. UV Spectra

The electronic spectra of the metal complex in methanol recorded in the UV region displayed intra ligand and charge transfer transitions. The spectra (Figure 5) showed three transitions in the ranges of 203-263 nm, 337 nm, and 384-386 nm, which can be assigned to $n\rightarrow\pi^*$, $\pi\rightarrow\pi^*$, and the charge transfer transitions (LMCT) from ligands to the metal, respectively. The spectra of metal complexes in chloroform recorded in the visible region showed transitions in the range of 400-420 nm, ascribed to charge transfer transition. Two transitions around 560-600 nm and 820-840 nm may be attributed to d-d transitions, which are characteristic of transition metal complexes [28-31]. It was clear that the UV-vis spectrum of the NiO nanoparticles was quite different from the starting complex, confirming the strong band that appeared at 350 nm was due to NiO

nanoparticles, not a Ni(II) complex [32,33]. In addition, the UV-vis spectrum of commercial bulk NiO powder does not show any observable absorption band [32].

3. FTIR Spectra

The IR spectrum showed five prominent bands in the ranges of 3400-3600, 2940, 1267-1212, 600-590, and 510 cm^{-1}, which may be assigned to the coordinated H_2O, N-H, CO, N–O, and M–N stretching vibrations, respectively. All bands of the *Aqua*(2-amino-6-methyl pyrimidine-4-ol and isoleucine)Ni(II) complex disappeared after thermal decomposition at 400 °C and a strong band at around 440 cm^{-1} was observed, which was assigned to the Ni–O stretching of the NiO NPs [33–37].

4. Thermal Studies

The thermal properties of the synthesized complex were investigated under an open atmosphere in the 0–800 °C temperature range with a heating rate of 10 °C/min using TG/DTA. Thermograms showed that the loss in weight corresponded to two water molecules in the temperature range 104-185 °C, followed by weight loss in the range 286-522 °C, which is approximately equal to the algebraic sum of weight loss due to HL and HP moieties [38-40]. The DTA of the complex (Figure 6) showed an endothermic peak in the range 104-185 °C, indicating the presence of coordinated water molecules, while a single exothermic peak in the range of 286-522 °C demonstrates the simultaneous decomposition of HL and HP moieties. The final main product (NiO) was confirmed by IR[41-42].

5. Scanning Electron Microscopy (SEM)

The SEM micrographs of the *Aqua* (2-amino-6-methyl pyrimidine-4-ol and isoleucine)Ni(II) complex and its decomposition product at 400 °C are presented in Figure 3. The powder form of the complex was composed of giant block crystals of different sizes (see Figure 3(a)). The SEM image of the product in Figure 3(b) shows that the shape and size of the particles were quite different from the precursor complex. The product consisted of extremely fine semi-spherical particles that were loosely aggregated. No characteristic morphology of the complex was observed, indicating complete decomposition into very fine spherical particles.

6. Transmission Electron Microscopy (TEM)

The TEM images of the complex and its decomposition product at 400 °C are shown in Figure 4. The starting complex powder was composed of very large block crystals of different sizes, as seen in Figure 4(a). The NiO nanoparticles formed after thermal decomposition of the complex were of uniform spherical shape, with weak agglomeration (Figure 4(b)). The particle sizes possessed a narrow distribution range from 10 to 18 nm, and the mean particle diameter was about 16 nm. The mean particle size determined by TEM was very close to the average particle size calculated by the Debye-Scherer formula from the XRD pattern.

7. X-ray diffraction analysis (XRD)

Powder XRD patterns of the *Aqua* (2-amino-6-methyl pyrimidine-4-ol and isoleucine)Ni(II) complex product after decomposition at 400 °C revealed only the diffraction peaks attributable to NiO with a face-centered cubic phase at 2θ = 37.40, 43.45, 62.95, 75.40 and 79.45 (Figure 2) which perfectly correlated to the (111), (200), (220), (311) and (222) crystal planes, respectively (JCPDS card No. 73-1523). This finding confirms that at 800 °C, the complex was entirely decomposed to nickel oxide. No impurity peaks were found in the XRD pattern, indicating that the nanocrystalline NiO obtained via this synthesis consisted of an ultrapure phase [43]. The average size of the NiO nanoparticles, estimated using the relative intensity peak (220) by the Debye-Scherrer equation, was found to be 16 nm, and the increase in sharpness of the XRD peaks indicated that the particles were crystalline in nature:

$$D=(094\lambda)/(\beta\cos\theta)$$

where λ is the wavelength (λ = 1.542 Å) (Cu-K_α), β is the full width at half maximum (FWHM) of the line, and θ is the diffraction angle.

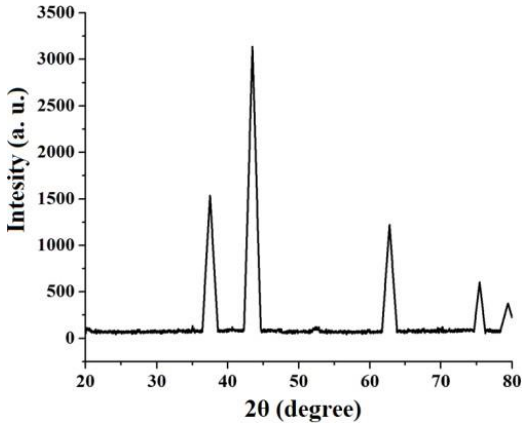

Figure 2. XRD pattern of the NiO nanoparticles

8. Antimicrobial Study

The studies based on the agar cup method revealed that the complex was sensitive against *C. diphtheriae*, but less sensitive against *C. Albicans* and *S. aureus* (Table 1). The minimum inhibitory concentration (MIC) of the complex ranged between 100-450 µg/mL. The biological study showed that the complex was more active against *C. diphtheriae* than *C. Albicans* and *S. aureus* compared to the standard antibacterial compound, doxycycline. The NiO NPs showed higher activity against the selected strains of microorganisms compared to the Ni(II) complex.

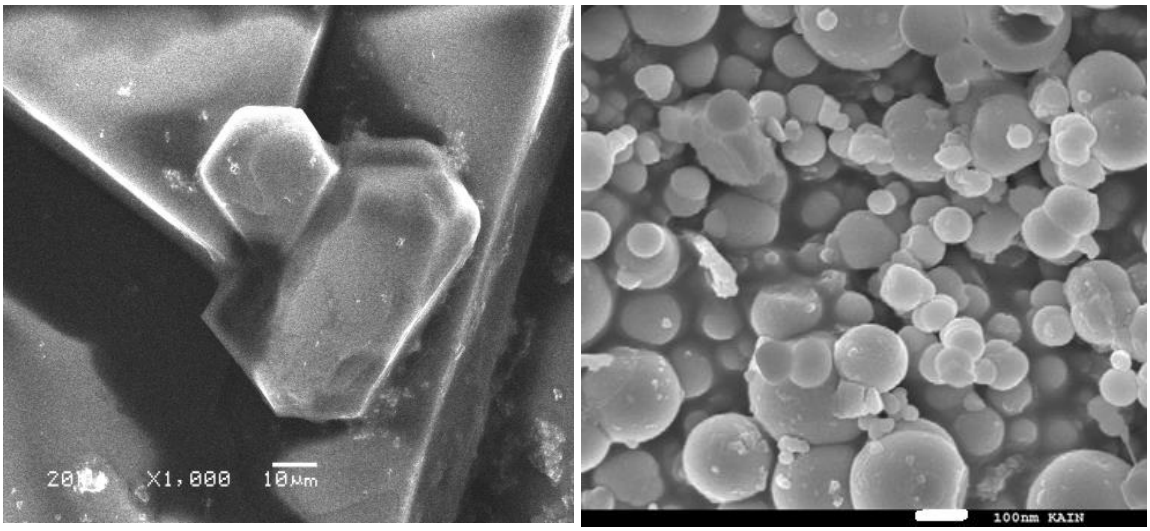

Figure 3. SEM micrographs of (**a**) *Aqua* (2-amino-6-methyl pyrimidine-4-ol and isoleucine) Ni(II) complex and (**b**) NiO nanoparticles.

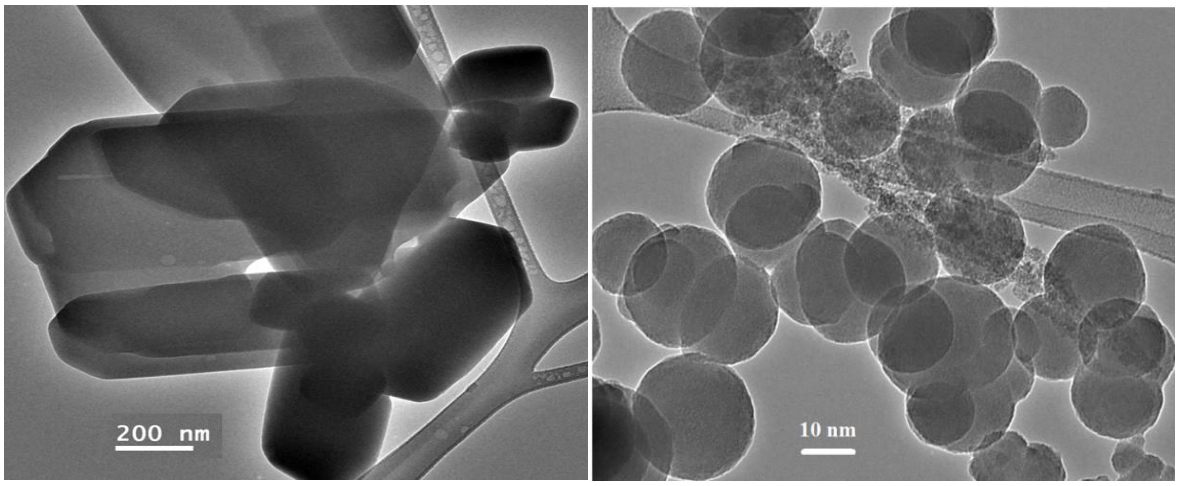

Figure 4. TEM micrographs of (**a**) *Aqua* (2-amino-6-methyl pyrimidine-4-ol and isoleucine) Ni(II) complex and (**b**) NiO nanoparticles

Table 1. Antibacterial activity of nickel (II) complex and NiO NPs by agar cup method (zone of inhibition (mm) and MIC (ug/mL))

No.	Complex	C. Albicans		S. diphtheriae		S. aureus	
		MIC (µg/mL)	(mm)	MIC (µg/mL)	(mm)	MIC (µg/mL)	(mm)
1	[Ni(P)(Iso).2H_2O]	160	15	150	14	300	14
2	NiO nanoparticles	500	18	100	20	150	18
3	Doxycycline	2.0	25	1.5	22	1.5	25

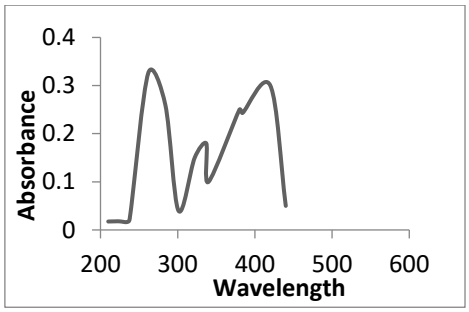

Figure 5. UV Spectra

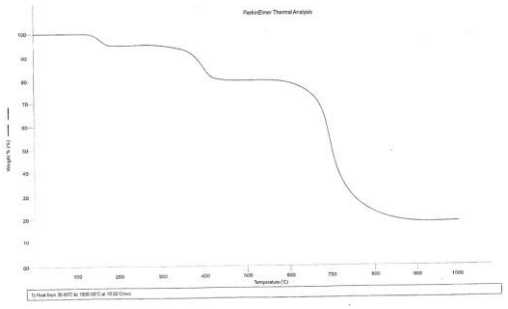

Figure 6. DTA Spectra

CONCLUSION

Ni(II) complex was subjected to thermal decomposition at a high temperature of 800 °C to obtain uniform spherical NiO nanoparticles in the range of 10–18 nm. The structure of the complex and the NiO nanoparticles produced were elucidated by FT-IR and UV-vis spectroscopy, TG/DTA, XRD, SEM, and TEM.

NiO nanoparticles showed an inhibitory effect against *C. diphtheriae*, *C. Albicans*, and *S. aureus* of 100-150 μg/mL, respectively. From these findings, we can conclude that the facile straightforward synthesis of NiO NPs has an advantage over other methods as it is simple, quick and energy-saving. The obtained NiO NPs also showed considerable activity against selected microorganisms compared to the Ni(II) complex.

ACKNOWLEDGEMENT

The authors are grateful to Prof. V. D. Barhate, Principal, Changu Kana Thakur Arts, Commerce and Science College (Autonomous), New Panvel for his continuous encouragement.

REFERENCES

1. Zollinger, H. (1991) Color chemistry: syntheses, properties and applications of organic dyes and pigments. *Weinheim: VCH*. https://doi.org/10.1002/anie.200385122

2. Motahari, F., Mozdianfard, M. R., Soofivand, F., et al. (2014) NiO nanostructures: Synthesis, characterization and photocatalyst application in dye wastewater treatment. *RSC Adv.*, **4(53)**, 27654–27660. https://doi.org/10.1039/C4RA02697G

3. Lin, S. H., Peng, C. F. (1996) Continuous treatment of textile wastewater by combined coagulation, electrochemical oxidation and activated sludge. *Water Res.*; **30(3)**, 587–592. https://doi.org/10.1016/0043-1354(95)00210-3

4. Din, M. I., Nabi, A. G., Rani, A., et al. (2018) Single step green synthesis of stable nickel and nickel oxide nanoparticles from Calotropis gigantea: catalytic and antimicrobial potentials. *Environ Nanotechnol Monit Manage*, **9**, 29–36. https://doi.org/10.1080/24701556.2019.1711401

5. Ahmed, S., Ahmad, M., Swami, B. L., et al. (2016) A review on plants extract mediated Synthesis of silver nanoparticles for anti-microbial applications: a green expertise. *J Adv Res*., **7(1)**, 17–28. https://doi.org/10.1016/j.jare.2015.02.007

6. Khan, M. S. J., Kamal, T., Ali, F., et al. (2019) Chitosan-coated polyurethane sponge supported metal nanoparticles for catalytic reduction of organic pollutants. *Int J Biol Macromol*., **132**, 772–783. https://doi.org/10.1016/j.ijbiomac.2019.03.205

7. Ali, F., Khan, S. B., Kamal, T., et al. (2018) Synthesis and characterization of M NPs templated chitosan-SiO2 catalyst for the reduction of nitrophenols and dyes. Carbohydr Polym., **192**, 217–230. https://doi.org/10.1016/j.carbpol.2018.03.029

8. Ali, N., Awais, Kamal, T., et al. (2018) Chitosan-coated cotton cloth supported copper nano-particles for toxic dye reduction. *Int J Biol Macromol.*, **111**, 832–838. https://doi.org/10.1016/j.ijbiomac.2018.01.092

9. Haider, A., Haider, S., Kang, I. -K., et al. (2018) A novel use of cellulose based filter paper containing silver nanoparticles for its potential application as wound dressing agent. *Int J Biol Macromol*., **108**, 455–461. https://doi.org/10.1016/j.ijbiomac.2017.12.022

10. Kamal, T., Khan, S. B., Haider, S., et al. (2017) Thin layer chitosancoated cellulose filter paper as substrate for immobilization of catalytic cobalt nanoparticles. *Int J Biol Macromol*., **104**, 56–62. https://doi.org/10.1016/j.ijbiomac.2017.05.157

11. Maniammal, K., Madhu, G., Biju, V. (2018) Nanostructured mesoporous NiO as an efficient photocatalyst for degradation of methylene blue:

structure, properties and performance. *Nano-Structures Nano-Objects*, **16**, 266–275. http://dx.doi.org/10.1016/j.nanoso.2018.07.007

12. Ruparelia, J. P., Chatterjee, A. K., Duttagupta, S. P. and Mukherji, S. (2008) Strain specificity in antimicrobial activity of Ag and Cu nanoparticles. *Acta Biomaterialia*, **4(3)**, 707–716. https://doi.org/10.1016/j.actbio.2007.11.006

13. Ren, G., Hu, D., Cheng, E. W. C., Vargas-Reus, M. A., Reip, P. and Allaker, R. P. (2009) Characterization of CuO nanoparticles for antimicrobial applications. *The International Journal of Antimicrobial Agents*, **33(6)**, 587–590. https://doi.org/10.1016/j.ijantimicag.2008.12.004

14. Yoon, K. Y., Byeon, J. H., Park, J. H. and Hwang, J. (2007) Susceptibility constants of Escherichia coli and Bacillus subtilis to Ag and Cu nanoparticles. *Science of the Total Environment*, **373(2-3)**, 572–575. https://doi.org/10.1016/j.scitotenv.2006.11.007

15. Davar, F., Fereshteh, Z., Salavati-Niasari, M. (2009) Nanoparticles Ni and NiO: Synthesis, characterization and magnetic properties. *J Alloys Compd.*, **476(1)**, 79. https://doi.org/10.1016/j.jallcom.2008.09.121

16. Song, X., Gao, L. (2008) Facile synthesis of polycrystalline NiO nanorods assisted by microwave heating. *J Am Ceram Soc.*, **91(10)**, 3465–3468. https://doi.org/10.1111/j.1551-2916.2008.02667.x

17. Li, Q., Wang, L. -S., Hu, B. -Y., et al. (2007) Preparation and characterization of NiO nanoparticles through calcination of malate gel. *Mater Lett.*, **61(8)**, 1615–1618. https://doi.org/10.1016/J.MATLET.2006.07.113

18. Li, J., Yan, R., Xiao, B., et al. (2008) Preparation of nano-NiO particles and evaluation of their catalytic activity in pyrolyzing biomass components. *Energy Fuels*, **22(1)**, 16–23. https://doi.org/10.1021/ef700283j

19. Wang, W. -N., Itoh, Y., Lenggoro, I. W., et al. (2004) Nickel and NiO nanoparticles prepared from nickel nitrate hexahydrate by a low pressure spray pyrolysis. *Mater Sci Eng B.*, **111(1)**, 69–76. http://dx.doi.org/10.1016/j.mseb. 2004.03.024

20. Wei, Z., Xia, T., Bai, L., et al. (2006) Efficient preparation for Ni nanopowders by anodic arc plasma. *Mater Lett.*, **60(6)**, 766–770. https://doi.org/10.1155/2009/795928

21. Chakrabarty, S., Chatterjee, K. (2009) Synthesis and characterization of nano-dimensional nickelous oxide (NiO) semiconductor. *J Phys Sci.*, **13**, 245–250. https://www.researchgate. net/publication/242595479_Synthesis_and_Characterization_of_Nano-Dimensional_Nickelous_Oxide_NiO_Semiconductor

22. Perrin, D. D., Perrin, D. R., Armarego, W. L. F. (1980) Purification of Laboratory Chemicals. *2nd ed., Pergamon Press Ltd., Oxford*.

23. Vogel, A. I. (1989) Textbook of Practical Organic Chemistry. *5th ed., Longmans Green and Co. Ltd., London*.

24. Weissberger, A. (1955) Techniques of Organic Chemistry, **7(2)**.

25. Jitendra M. Pawara and Sunil S. Patil (2021) An Innovative Method Designed for the Synthesis of Some New Mixed Ligand Ni(II) Complexes Its Characterization and Applications. *World Journal of Chemical Education*, **9(2)**, 50-56. doi: 10.12691/wjce-9-2-3.

26. Liberta, A. E. and West, D. X. (1992) Antifungal and antitumor activity of heterocyclic thiosemicarbazones and their metal complexes: current status. *Biometals S.*, **5(2)**, 121–126. DOI: 10.1007/978-94-011-5780-3_29

27. Geary, W. J. (1971) *Coord. Chem. Rev*., **7**, 81. http://dx.doi.org/10.1016/S0010-8545(00)80009-0

28. Tumer, M. (2000) Synth. React. Inorg. *Met.-Org. Chem*., **30**, 1139. https://doi.org/10.1007/s11243-006-0087-0

29. Chakrawarti, P. B., Khanna, P. (1985) *J. Ind. Chem. Soc.*, **77**, 23 D. DOI: 10.1007/978-3-662-08178-5_3

30. Beraldo, H., Kainser, S. M., Turner, J. D., Billeh, I. S., Ives, J. S., West, D. X. (2007) *Trans. Metal Chem.*, **22**, 528. DOI: 10.12691/wjce-9-2-3

31. Lever, A. B. (1974) *J. Chem. Educ.*, **51**, 612. https://doi.org/10.1021/ed051p612

32. Salavati-Niasari, M., Mohandes, F., Davar, F., Mazaheri, M., Monemzadeh, M., Yavarinia, N. (2009) Preparation of NiO nanoparticles from metal-organic frameworks via a solid-state decomposition route. *Inorg. Chim. Acta*, **362**, 3691–3697. https://dx.doi.org/10.3390%2Fijms141223941

33. Salavati-Niasari, M., Mir, N., Davar, F. (2009) Synthesis and characterization of NiO nanoclusters via thermal decomposition. *Polyhedron*, **28**, 1111–1114. http://dx.doi.org/ 10.1016/j.poly.2009.01.026

34. Wellington, K. W., Kaye, P. T., Watkinsa, G. M. (2008) Designer ligands. Part 14. Novel Mn(lI), Ni(II) and Zn(II) complexes of benzamide- and

biphenyl-derived ligands. *Arch. Org. Chem*., **17**, 248–264. http://hdl.handle.net/10204/3252

35. Lai, S., Hsiao, C., Ling, J., Wang, W., Peng, S., Chen, I. (2008) Metal–metal bonding in metal-string complexes M3(dpa)4X2 (M = Ni, Co, dpa = di(2-pyridyl)amido, and X = Cl, NCS) from resonance Raman and infrared spectroscopy. *Chem. Phys. Lett.*, **456**, 181–185. http://dx.doi.org/10.1016%2Fj.cplett.2008.03.050

36. Wang, C., Shao, C., Wang, L., Zhang, L., Li, X., Liu, Y. (2009) Electrospinning preparation, characterization and photocatalytic properties of Bi2O3 nanofibers. *J. Colloid Interface Sci*., **333**, 242–248. https://doi.org/10.1039/C4RA03754E

37. Warad, I., Hammouti, B., Hadda, T. B., Boshaala, A., Haddad, S. F. (2013) X-ray single-crystal structure of a novel di-μ-chloro-bis[chloro(2,9-dimethyl-1,10 phenanthroline)nickel(II)] complex: Synthesis, and spectral and thermal studies. *Res. Chem. Intermed.*, **39**, 4011–4020. https://doi.org/10.1155/2014/914241

38. Bailey, R. A., Kozak, S. L., Michelson, T. W., Mills, W. N. (1971) *Coord. Chem. Rev*., **6**, 407. https://doi.org/10.1016/S0010-8545(00)80015-6

39. Holm, R. H., Cornor, M. J. O. (1971) *Prog. Inorg. Chem.*, **14**, 241. https://doi.org/10.1021/ic991048k

40. Dash, K. C., Mohanta, H. N. (1977) *J. Inorg. Nucl. Chem*., **39**, 1345. https://doi.org/10.1016/S0020-1693(00)84854-9

41. Shivankar, V. S., Dharwadkar, S. R., Thakkar, N. V. (2002) Proceedings of the 13th National Symposium on Thermal Analysis (THERMANS 2002), **52**. http://www.dmclibrary.yolasite.com/resources/Thermochim_acta%20(1).pdf

42. Prasad, R. V., Thakkar N. V. (1994) *J. Mol. Catal.*, **92**, 9. https://doi.org/10.1016/0304-5102(94)00063-8

43. Klug, H. P., Alexander, L. E. (1964) X-ray Diffraction Procedures, 2nd ed.; Wiley: New York, NY, USA. https://doi.org/10.1002/bbpc.19750790622